

High-efficiency fluorescent organic light-emitting diodes enabled by triplet-triplet annihilation and horizontal emitter orientation

Christian Mayr, Tobias D. Schmidt, Wolfgang Brütting

Angaben zur Veröffentlichung / Publication details:

Mayr, Christian, Tobias D. Schmidt, and Wolfgang Brütting. 2014.
“High-efficiency fluorescent organic light-emitting diodes enabled by triplet-triplet annihilation and horizontal emitter orientation.” Applied Physics Letters 105 (18): 183304. <https://doi.org/10.1063/1.4901341>.

Nutzungsbedingungen / Terms of use:

licgercopyright

Dieses Dokument wird unter folgenden Bedingungen zur Verfügung gestellt: / This document is made available under the following conditions:

Deutsches Urheberrecht

Weitere Informationen finden Sie unter: / For more information see:

<https://www.uni-augsburg.de/de/organisation/bibliothek/publizieren-zitieren-archivieren/publizieren>



High-efficiency fluorescent organic light-emitting diodes enabled by triplet-triplet annihilation and horizontal emitter orientation

Cite as: Appl. Phys. Lett. **105**, 183304 (2014); <https://doi.org/10.1063/1.4901341>

Submitted: 24 September 2014 . Accepted: 29 October 2014 . Published Online: 06 November 2014

Christian Mayr, Tobias D. Schmidt, and Wolfgang Brütting



View Online



Export Citation



CrossMark

ARTICLES YOU MAY BE INTERESTED IN

[Organic electroluminescent diodes](#)

Applied Physics Letters **51**, 913 (1987); <https://doi.org/10.1063/1.98799>

[Efficient up-conversion of triplet excitons into a singlet state and its application for organic light emitting diodes](#)

Applied Physics Letters **98**, 083302 (2011); <https://doi.org/10.1063/1.3558906>

[Determination of molecular dipole orientation in doped fluorescent organic thin films by photoluminescence measurements](#)

Applied Physics Letters **96**, 073302 (2010); <https://doi.org/10.1063/1.3309705>

Lock-in Amplifiers

... and more, from DC to 600 MHz



High-efficiency fluorescent organic light-emitting diodes enabled by triplet-triplet annihilation and horizontal emitter orientation

Christian Mayr,^{a)} Tobias D. Schmidt, and Wolfgang Brütting^{b)}
Institute of Physics, University of Augsburg, 86135 Augsburg, Germany

(Received 24 September 2014; accepted 29 October 2014; published online 6 November 2014)

A green organic light-emitting diode with the fluorescent emitter Coumarin 545T shows an external quantum efficiency (η_{EQE}) of 6.9%, clearly exceeding the classical limit of 5% for fluorescent emitters. The analysis of the angular dependent photoluminescence spectrum of the emission layer reveals that 86% of the transition dipole moments are horizontally oriented. Furthermore, transient electroluminescence measurements demonstrate the presence of a delayed emission originating from triplet-triplet annihilation. A simulation based efficiency analysis reveals quantitatively the origin for the high η_{EQE} : a radiative exciton fraction higher than 25% and a light-outcoupling efficiency of nearly 30%. © 2014 AIP Publishing LLC. [<http://dx.doi.org/10.1063/1.4901341>]

Since the development of the first efficient organic light-emitting diodes (OLEDs) in the 1980s,¹ research has made significant progress. In addition to their application in general lighting, OLEDs have found their way into everyday life, especially employed in displays. Consisting of a layered structure, a bias is applied to an OLED to inject and transport electrons and holes from the cathode and anode, respectively, to the emission layer, where they recombine, form excitons, and decay under the emission of photons. With the appropriate choice of the emitting molecules, the color of an OLED device can be tuned almost arbitrarily. The dye in the emission layer also has a major influence on the quantum efficiency (i.e., the ratio of the number of emitted photons to injected electrons) of OLEDs—beside the transport layers governing the electrical properties. The probability for a radiative decay of an excited state of an emitter molecule is characterized by its radiative quantum efficiency q . The fraction of excitons that are allowed to decay radiatively (η_r) concerning quantum mechanical selection rules is 25% for fluorescent^{2,3} and 100% for phosphorescent⁴⁻⁶ emitters, facilitating efficient spin-orbit coupling, respectively. Being in a multilayer structure with different refractive indices, the light-outcoupling efficiency η_{out} is mainly governed by the OLED stack design and has been estimated to be at most 20% for a long time.⁷ Together with the charge carrier balance γ , the external quantum efficiency η_{EQE} is defined as the product of these individual factors⁸

$$\eta_{\text{EQE}} = \gamma \times \eta_r \times q_{\text{eff}} \times \eta_{\text{out}} = \eta_{\text{int}} \times \eta_{\text{out}}. \quad (1)$$

In this equation, η_{int} represents the internal quantum efficiency. q_{eff} is the effective radiative quantum efficiency, derived from the (intrinsic) radiative quantum efficiency q by a modification induced by the OLED cavity due to the Purcell effect.⁹⁻¹² Classical limits for η_{EQE} of 5% for fluorescent and 20% for phosphorescent emitters, respectively, have been stated following the assumptions made above, however, recent reports about efficiencies exceeding these

limitations have been published: Delayed fluorescence, originating from triplet-triplet annihilation (TTA)¹³⁻¹⁸ or thermally activated delayed fluorescence (TADF),¹⁹⁻²⁴ increases the radiative exciton fraction beyond 25% and has been identified as one reason for these high efficiencies. By using TADF emitters, comparable efficiencies to phosphorescent OLEDs can be realized.²⁵⁻²⁷ Only recently, our group^{28,29} and others¹⁶ have shown that in addition to the increased radiative exciton fraction in OLEDs showing delayed fluorescence, also horizontal orientation of the transition dipole moments of the emitting molecules is responsible for this high efficiency. The reason for this behavior is the reduced coupling to surface plasmons with the accompanied enhancement of the light-outcoupling efficiency.^{30,31} The incorporation of emitters having horizontally oriented transition dipole moments in OLEDs has the potential to boost η_{EQE} by a factor of more than 1.5 compared to isotropic orientation.³¹⁻³³ Especially for phosphorescent OLEDs with (partial) horizontal orientation of the emitter molecules, record efficiencies with η_{EQE} exceeding 30% have been reported recently.³³⁻³⁵ Thus, for an efficiency analysis, the knowledge of the orientation of the transition dipole moments of the emitter is crucial and leads to implications for the determination of the other constituting factors of η_{EQE} according to Eq. (1). Especially, if η_{out} is underestimated (due to ignoring horizontal emitter orientation), the determined radiative exciton fraction will be too high for emitters showing delayed fluorescence, since only the η_{EQE} of an OLED device and the radiative quantum efficiency q are directly accessible by experiments.^{28,29}

In this letter, we analyze the orientation of the transition dipole moments of the widely used fluorescent green emitter 2,3,6,7-tetrahydro-1,1,7,7-tetramethyl-1H,5H,11H-10-(2-benzothiazolyl)quinolizino[9,9a,1gh]coumarin (C545T). Furthermore, quantifying the contributions of both an increase of the light-outcoupling efficiency η_{out} due to non-isotropic emitter orientation as well as a TTA-induced enhancement of the radiative exciton fraction η_r leads to a comprehensive understanding of the η_{EQE} in OLED devices.

C545T is a very efficient fluorescent emitter, and OLEDs with efficiencies higher than the classical limit of 5% have

^{a)}Christian.Mayr@physik.uni-augsburg.de

^{b)}Wolfgang.Brueetting@physik.uni-augsburg.de

already been reported.^{17,36} This high efficiency has been attributed to an enhanced radiative exciton fraction originating from TTA. However, there are indications that possibly a higher light-outcoupling efficiency than the assumed 20% prevails in OLEDs using this emitting system: For example, in the analysis performed by Pu *et al.*,¹⁷ there is a discrepancy between the determined radiative exciton fraction of 54% (derived from the measured η_{EQE} by assuming 20% light-outcoupling efficiency η_{out}), which is very close to the theoretical maximum of 62.5% for a TTA emitter,¹⁴ and the time-resolved electroluminescence (EL) responses (comparison between the EL-intensity under steady-state conditions and delayed fluorescence) suggesting a radiative exciton fraction η_r of only $\sim 1.25 \times 25\% = 31.3\%$. In that report, it was also speculated that C545T shows anisotropic emitter orientation. Unfortunately, due to the insensitivity of variable angle spectroscopic ellipsometry (VASE) to small portions of guest molecules in a host, no information about its orientation could be obtained.

In order to measure the degree of horizontal emitter orientation of C545T, we have analyzed the angular dependent p-polarized photoluminescence (PL) emission of 15 nm Aluminium-tris(8-hydroxyquinolin) (Alq_3) doped with C545T (1 wt. %).³⁷ The film has been deposited on a glass substrate, attached to a fused silica prism, excited by a 375 nm cw laser diode at 45° incident angle and mounted on a rotation stage. The spectra were measured using a fibre optical spectrometer (SMS-500, Sphere Optics) and a polarizing filter to distinguish between p- and s-polarized light. The p-polarized emission includes contributions of the horizontal p_x and vertical p_z transition dipole moments. The degree of orientation is characterized by an anisotropy factor Θ (fraction of the number of vertically oriented to the total number of transition dipole moments).³⁸ By comparing the measurement with the result of optical simulations, information about the ratio of horizontal and vertical transition dipole moments can be obtained. The s-polarized emission only

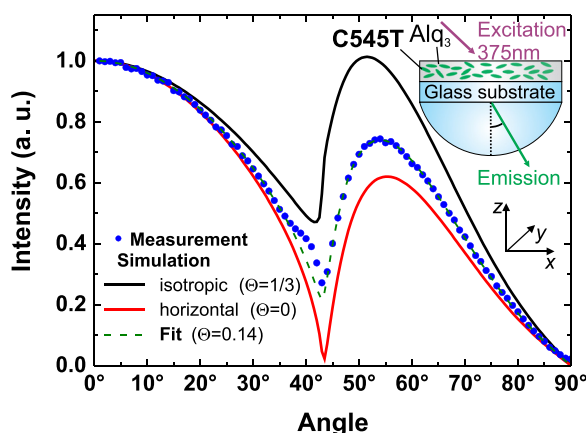


FIG. 1. Cross-section of the angular dependent p-polarized PL emission spectra of 15 nm Alq_3 doped with C545T (1 wt. %) on a glass substrate at a wavelength of 523 nm (The polarization of light is given with respect to an observer in the x - z -plane.). The black and the red curves represent the simulation for perfectly isotropic ($\Theta = 1/3$) and horizontal ($\Theta = 0$) orientation of the transition dipole moments, respectively. The measured data have been fitted (green dashed line) to an orientation of $\Theta = 0.14$, corresponding to 86% horizontally oriented transition dipole moments in the film. The emission intensity has been normalized to the emission at an angle of 0°.

contains contributions of the p_y dipole, and thus, no information about emitter orientation can be extracted. The simulation calculates the power distribution of radiating dipoles to different optical modes in a multilayer stack and is based on a transfer-matrix formalism.³⁹ In Fig. 1, the measured and calculated angular-dependent p-polarized emission into the glass substrate is shown as a cross-section at a wavelength of 523 nm. The measurement reveals significant anisotropic orientation of the transition dipole moments of the emitter with an almost perfect fit for an anisotropy factor of $\Theta = 0.14$, corresponding to 86% horizontally oriented transition dipole moments.

OLEDs have been fabricated with optimized film thicknesses for maximum light-outcoupling (by performing optical simulations taking the non-isotropic emitter orientation into account) with the following stack: Glass/130 nm ITO/1 nm WO_3 /30 nm CBP/30 nm C545T: Alq_3 (1 wt. %)/27 nm Alq_3 /0.8 nm LiF/100 nm Al. This stack layout has the advantage of having a direct hole injection into the highest occupied molecular orbital of 4,4'-Bis(carbazol-9-yl)bi-phenyl (CBP) and no interfaces for holes to accumulate at.⁴⁰ In Fig. 2, measured current density-voltage characteristics, EL spectrum, and η_{EQE} as a function of the current density are shown. The OLED shows a green emission with a peak

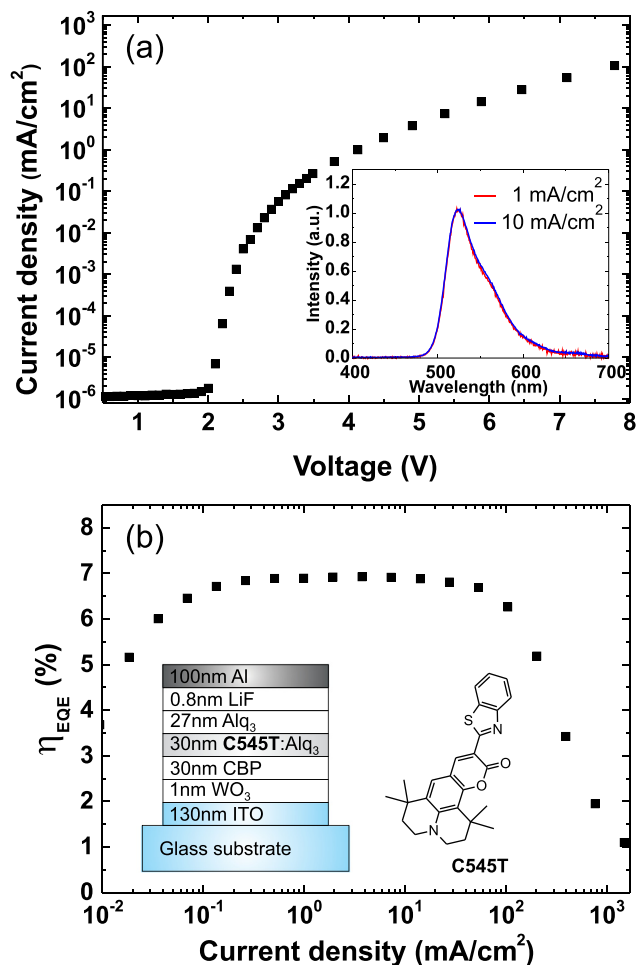


FIG. 2. (a) Current density-voltage characteristics (inset: EL spectrum) and (b) measured external quantum efficiency η_{EQE} as a function of the current density for the stack shown in the inset.

intensity at 523 nm. External quantum efficiencies have been measured in a calibrated integrating sphere.⁴¹

The η_{EQE} reaches values close to 7% and remains nearly constant in a remarkably broad range of current densities extending from about 0.1 to almost 100 mA/cm². This indicates that charge carrier balance is close to 100% in this device. The achieved maximum η_{EQE} of 6.9% exceeds the classical limit of 5% by far, which is in good agreement with previously published data.⁴⁰ The drop in η_{EQE} for current densities below 0.1 mA/cm² and above 100 mA/cm² can be ascribed to non-perfect charge carrier balance and to quenching of excitons caused by interaction with charges or other excited molecules, respectively.⁴²

OLEDs with C545T are known to show delayed fluorescence from TTA.¹⁵ Thus, time-resolved spectra of the EL have been recorded with a streak camera system (Hamamatsu C5680) and a spectrograph (Princeton Instruments Acton SpectraPro 2300i). Electrical excitation was established by an arbitrary waveform generator (Tabor Electronics WW2571A) applying a 50 μs square wave voltage pulse with variable bias to the OLED. Additionally, to prevent the recombination of trapped charges, a negative reverse bias of <-4 V has been applied just after the forward bias pulse. A delayed component originating from TTA can be observed after switching off the forward bias pulse (Fig. 3). The curves—which were normalized to the intensity at steady-state conditions—are almost identical, which is consistent to the η_{EQE} characteristics, implying a constant contribution from TTA to the η_{EQE} in a wide current-density range. By comparing the intensity of the (extrapolated) delayed component to the total intensity under steady-state conditions, an enhancement factor of the radiative exciton fraction of ~ 1.18 can be determined, suggesting a radiative exciton fraction η_r of $\sim 29.5\%$.

With the knowledge of the orientation of the transition dipole moments of C545T, it is possible to calculate the light-outcoupling efficiency η_{out} of the OLED by optical simulations. In Fig. 4, the experimental η_{EQE} for two OLEDs with different Alq₃ thicknesses is compared with optical simulations (see supplementary material for used

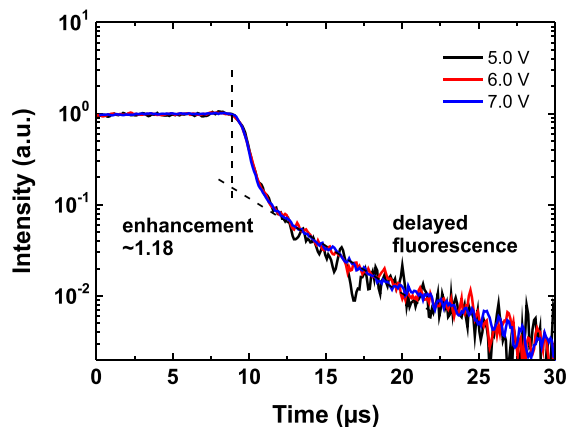


FIG. 3. Transient EL response integrated over the emission spectrum for the OLED stack shown in Fig. 2(b) for varying excitation pulses. Delayed fluorescence is observable causing an enhancement of the total EL intensity by a factor of ~ 1.18 . The lifetime of the delayed component is much longer than the initial drop of the RC-time of the device (~ 1 μs).

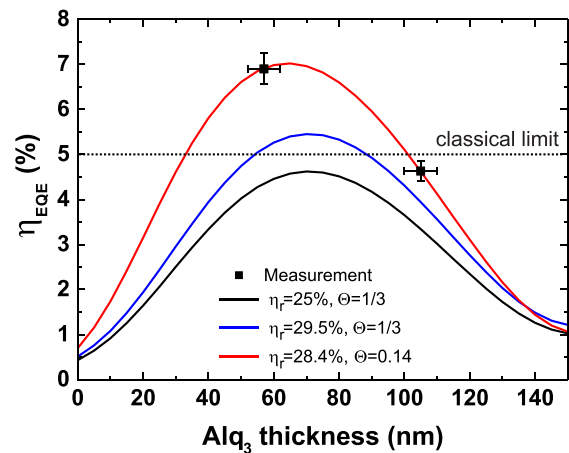


FIG. 4. Measured η_{EQE} for two OLEDs with Alq₃ thicknesses of 57 nm and 105 nm compared to optical simulations. Assuming a perfect charge balance factor ($\gamma = 1$), isotropic emitter orientation ($\Theta = 1/3$) and disregarding delayed fluorescence from TTA ($\eta_r = 0.25$), a maximum η_{EQE} of only 4.3% for an OLED with 57 nm Alq₃ thickness can be anticipated (black curve). Taking the delayed fluorescence into account and assuming $\eta_r = 1.18 \times 25\% = 29.5\%$, as estimated from transient EL, the η_{EQE} can be increased only up to 5.1% (blue curve) for the mentioned Alq₃ thickness of 57 nm. By taking the horizontal orientation of the transition dipole moments of the emitter C545T into account ($\Theta = 0.14$), the experimental result can be explained by an increased light-outcoupling efficiency ($\eta_{\text{out}} = 29.9\%$) and delayed fluorescence ($\eta_r = 1.14 \times 25\% = 28.4\%$) (red curve).

optical constants⁴³). For the calculation, a charge balance factor $\gamma = 1$ and a radiative quantum efficiency of $q = 0.77$ (calculated from the measured value of the PL quantum efficiency $\phi_{\text{PL}} = 0.8$ (Ref. 44) by taking the light-outcoupling and Purcell effect into account²⁹) have been assumed. The calculation of the η_{EQE} for an isotropically oriented emitter ($\eta_{\text{out}} = 21.0\%$) with no delayed component ($\eta_r = 25\%$, black curve) cannot explain the experimental result. The same applies to an isotropically oriented emitter with a delayed component enhancing the radiative exciton fraction as estimated from the transient EL responses ($\eta_r = 29.5\%$, blue curve). Taking the actual light-outcoupling efficiency $\eta_{\text{out}} = 29.9\%$ into account, which is higher due to the horizontal orientation of the transition dipole moments of the emitter and treating η_r as a free parameter, the simulation matches the measurement by identifying $\eta_r \geq 28.4\%$ (assuming $\gamma \sim 1$). Thus, the precise knowledge of the light-outcoupling efficiency allows to determine the value of the radiative exciton fraction. This value is consistent to the estimation obtained by a direct measurement of the transient EL response. However, assuming an isotropic emitter orientation would result in an overestimation of the radiative exciton fraction. From the conducted efficiency analysis, the contribution of horizontal emitter orientation and delayed fluorescence originating from TTA to the enhanced η_{EQE} can be quantified: horizontal orientation boosts the efficiency by 39.8% (compared to isotropic orientation) and the delayed fluorescence by 14% (compared to a purely fluorescent emitter). Thus, the increased light-outcoupling efficiency η_{out} is playing the major role for OLEDs comprising the analyzed emitting system. This emphasizes the impact of horizontal emitter orientation in fluorescent OLEDs exceeding the classical limit for η_{EQE} , which

would otherwise be incorrectly attributed exclusively to delayed fluorescence and internal quantum efficiency η_{int} .

In summary, we have shown that the transition dipole moments of the fluorescent emitter C545T doped in Alq₃ adopt strong horizontal orientation. OLEDs with this emitter system have been fabricated showing an η_{EQE} of 6.9%, which is exceeding the classical limit. By performing an efficiency analysis, $\eta_{\text{r}} \geq 28.4\%$ and $\eta_{\text{out}} = 29.9\%$ were obtained. The impact of delayed fluorescence originating from TTA would have been significantly overestimated, if isotropic emitter orientation was assumed instead. Additionally, these numbers give clues for the development of new high efficiency emitters, demonstrating potentials for further improvement.

We acknowledge financial support by Bayerische Forschungsförderung and Deutsche Forschungsgemeinschaft (Contract No. BR 1728/13-1). We want to thank Daniel Fluhr for technical support regarding integrating sphere measurements.

- ¹C. W. Tang and S. A. VanSlyke, *Appl. Phys. Lett.* **51**, 913 (1987).
- ²M. A. Baldo, D. F. O'Brien, M. E. Thompson, and S. R. Forrest, *Phys. Rev. B* **60**, 14422–14428 (1999).
- ³M. Segal, M. A. Baldo, R. J. Holmes, S. R. Forrest, and Z. G. Soos, *Phys. Rev. B* **68**, 075211 (2003).
- ⁴M. A. Baldo, D. F. O'Brien, Y. You, A. Shoustikov, S. Sibley, M. E. Thompson, and S. R. Forrest, *Nature* **395**, 151–154 (1998).
- ⁵J. S. Wilson, A. S. Dhoot, A. J. A. B. Seeley, M. S. Khan, A. Köhler, and R. H. Friend, *Nature* **413**, 828–831 (2001).
- ⁶Y. Sun, N. C. Giebink, H. Kanno, B. Ma, M. E. Thompson, and S. R. Forrest, *Nature* **440**, 908–912 (2006).
- ⁷N. C. Greenham, R. H. Friend, and D. D. C. Bradley, *Adv. Mater.* **6**, 491–494 (1994).
- ⁸T. Tsutsui, E. Aminaka, C. P. Lin, and D. U. Kim, *Philos. Trans. R. Soc. London* **355**, 801–814 (1997).
- ⁹S. Nowy, B. C. Krummacker, J. Frischeisen, N. A. Reinke, and W. Brütting, *J. Appl. Phys.* **104**, 123109 (2008).
- ¹⁰H. Becker, S. E. Burns, and R. H. Friend, *Phys. Rev. B* **56**, 1893–1905 (1997).
- ¹¹B. C. Krummacker, S. Nowy, J. Frischeisen, M. Klein, and W. Brütting, *Org. Electron.* **10**, 478–485 (2009).
- ¹²X.-W. Chen, W. C. H. Choy, C. J. Liang, P. K. A. Wai, and S. He, *Appl. Phys. Lett.* **91**, 221112 (2007).
- ¹³D. Y. Kondakov, *J. Appl. Phys.* **102**, 114504 (2007).
- ¹⁴D. Y. Kondakov, T. D. Pawlik, T. K. Hatwar, and J. P. Spindler, *J. Appl. Phys.* **106**, 124510 (2009).
- ¹⁵Y. Luo and H. Aziz, *Adv. Funct. Mater.* **20**, 1285–1293 (2010).
- ¹⁶D. Yokoyama, Y. Park, B. Kim, S. Kim, Y.-J. Pu, J. Kido, and J. Park, *Appl. Phys. Lett.* **99**, 123303 (2011).
- ¹⁷Y.-J. Pu, G. Nakata, F. Satoh, H. Sasabe, D. Yokoyama, and J. Kido, *Adv. Mater.* **24**, 1765–1770 (2012).
- ¹⁸T. Suzuki, Y. Nonaka, T. Watabe, H. Nakashima, S. Seo, S. Shitagaki, and S. Yamazaki, *Jpn. J. Appl. Phys.* **53**, 052102 (2014).
- ¹⁹A. Endo, M. Ogasawara, A. Takahashi, D. Yokoyama, Y. Kato, and C. Adachi, *Adv. Mater.* **21**, 4802–4806 (2009).
- ²⁰A. Endo, K. Sato, K. Yoshimura, T. Kai, A. Kawada, H. Miyazaki, and C. Adachi, *Appl. Phys. Lett.* **98**, 083302 (2011).
- ²¹R. Czerwieńiec, J. Yu, and H. Yersin, *Inorg. Chem.* **50**, 8293–8301 (2011).
- ²²S. Y. Lee, T. Yasuda, H. Nomura, and C. Adachi, *Appl. Phys. Lett.* **101**, 093306 (2012).
- ²³H. Uoyama, K. Goushi, K. Shizu, H. Nomura, and C. Adachi, *Nature* **492**, 234–238 (2012).
- ²⁴Q. Zhang, B. Li, S. Huang, H. Nomura, H. Tanaka, and C. Adachi, *Nature Photon.* **8**, 326–332 (2014).
- ²⁵Y. J. Cho, K. S. Yook, and J. Y. Lee, *Adv. Mater.* **26**, 4050–4055 (2014).
- ²⁶B. S. Kim and J. Y. Lee, *Adv. Funct. Mater.* **24**, 3970–3977 (2014).
- ²⁷J. W. Sun, J.-H. Lee, C.-K. Moon, K.-H. Kim, H. Shin, and J.-J. Kim, *Adv. Mater.* **26**, 5684–5688 (2014).
- ²⁸T. D. Schmidt, D. S. Setz, M. Flämmich, J. Frischeisen, D. Michaelis, C. Mayr, A. F. Rausch, T. Wehler, B. J. Scholz, T. C. G. Reusch, N. Danz, and W. Brütting, *Appl. Phys. Lett.* **103**, 093303 (2013).
- ²⁹C. Mayr, S. Y. Lee, T. D. Schmidt, T. Yasuda, C. Adachi, and W. Brütting, *Adv. Funct. Mater.* **24**, 5232–5239 (2014).
- ³⁰W. H. Weber and C. F. Eagen, *Opt. Lett.* **4**, 236 (1979).
- ³¹J. Frischeisen, D. Yokoyama, A. Endo, C. Adachi, and W. Brütting, *Org. Electron.* **12**, 809–817 (2011).
- ³²M. Flämmich, J. Frischeisen, D. S. Setz, D. Michaelis, B. C. Krummacker, T. D. Schmidt, W. Brütting, and N. Danz, *Org. Electron.* **12**, 1663–1668 (2011).
- ³³S.-Y. Kim, W.-I. Jeong, C. Mayr, Y.-S. Park, K.-H. Kim, J.-H. Lee, C.-K. Moon, W. Brütting, and J.-J. Kim, *Adv. Funct. Mater.* **23**, 3896–3900 (2013).
- ³⁴K.-H. Kim, C.-K. Moon, J.-H. Lee, S.-Y. Kim, and J.-J. Kim, *Adv. Mater.* **26**, 3844–3847 (2014).
- ³⁵K.-H. Kim, S. Lee, C.-K. Moon, S.-Y. Kim, Y.-S. Park, J.-H. Lee, J. W. Lee, J. Huh, Y. You, and J.-J. Kim, *Nat. Commun.* **5**, 4769 (2014).
- ³⁶K. Okumoto, H. Kanno, Y. Hamaa, H. Takahashi, and K. Shibata, *Appl. Phys. Lett.* **89**, 063504 (2006).
- ³⁷J. Frischeisen, D. Yokoyama, C. Adachi, and W. Brütting, *Appl. Phys. Lett.* **96**, 073302 (2010).
- ³⁸T. D. Schmidt, D. S. Setz, M. Flämmich, J. Frischeisen, D. Michaelis, B. C. Krummacker, N. Danz, and W. Brütting, *Appl. Phys. Lett.* **99**, 163302 (2011).
- ³⁹W. Brütting, J. Frischeisen, T. D. Schmidt, B. J. Scholz, and C. Mayr, *Phys. Status Solidi A* **210**, 44–65 (2013).
- ⁴⁰Z. B. Wang, M. G. Helander, J. Qiu, Z. W. Liu, M. T. Greiner, and Z. H. Lu, *J. Appl. Phys.* **108**, 024510 (2010).
- ⁴¹S. Forrest, D. Bradley, and M. Thompson, *Adv. Mater.* **15**, 1043–1048 (2003).
- ⁴²Y. Zhang and S. R. Forrest, *Phys. Rev. Lett.* **108**, 267404 (2012).
- ⁴³See supplementary material at <http://dx.doi.org/10.1063/1.4901341> for optical constants.
- ⁴⁴M. Tian, J. Luo, and X. Liu, *Opt. Express* **17**, 21370–21375 (2009).